

NONNUCLEAR HYPER/ULTRALUMINOUS X-RAY SOURCES IN THE STARBURSTING CARTWHEEL RING GALAXY

YU GAO,¹ Q. DANIEL WANG,¹ P. N. APPLETON,² AND RAY A. LUCAS³

Received 2003 June 27; accepted 2003 September 5; published 2003 September 29

ABSTRACT

We report the *Chandra*/ACIS-S detection of more than 20 ultraluminous X-ray sources (ULXs; $L_{0.5-10\text{ keV}} \gtrsim 3 \times 10^{39}$ ergs s⁻¹) in the Cartwheel collisional ring galaxy system, of which over a dozen are located in the outer active star-forming ring. A remarkable hyperluminous X-ray source (HLX; $L_{0.5-10\text{ keV}} \gtrsim 10^{41}$ ergs s⁻¹ assuming isotropic radiation), which dominates the X-ray emission from the Cartwheel ring, is located in the same segment of the ring as most ULXs. These powerful H/ULXs appear to be coincident with giant H II region complexes, young star clusters, and radio and mid-infrared hot spots: all strong indicators of recent massive star formation. The X-ray spectra show that H/ULXs have similar properties as those of the *most luminous* ULXs found in the nearest starbursts and galaxy mergers such as the Antennae galaxies and M82. The close association between the X-ray sources and the starbursting ring strongly suggests that the H/ULXs are intimately associated with the production and rapid evolution of short-lived massive stars. The observations represent the most extreme X-ray luminosities discovered to date associated with star-forming regions—rivaling the X-ray luminosities usually associated with active galactic nuclei.

Subject headings: galaxies: active — galaxies: individual (Cartwheel, VV 784) — galaxies: interactions — galaxies: starburst — X-rays: galaxies

On-line material: color figures

1. INTRODUCTION

The high-resolution capabilities of *Chandra* have led to the discovery of a large population of extraordinarily X-ray-luminous pointlike nonnuclear sources in many nearby galaxies (e.g., Fabianno, Zezas, & Murray 2001; Colbert et al. 2003). These so-called ultraluminous X-ray sources (ULXs; Makishima et al. 2000) can have apparent isotropic broadband X-ray luminosities of $L_{0.5-10\text{ keV}}$: hundreds of times the Eddington limit for a neutron star or a stellar mass black hole. Although rarely present in normal galaxies, very luminous ULXs with $L_{0.5-10\text{ keV}} \gtrsim 3 \times 10^{39}$ ergs s⁻¹ are often found in starbursts and IR-luminous galaxy mergers. For example, in both the Antennae galaxies and the luminous IR galaxy merger NGC 3256, more than half a dozen such luminous ULXs are detected (Fabianno et al. 2001; Lira et al. 2002), and numerous less luminous pointlike sources are spread over the merging disks (Zezas et al. 2002). The *Chandra* observations of the Cartwheel galaxy⁴ presented here show an unusually large number (greater than 20) of high-luminosity ULXs, most of which appear highly correlated with the narrow, young, outer starburst ring.

Hyperluminous X-ray sources (HLXs; $L_{0.5-10\text{ keV}} \gtrsim 10^{41}$ ergs s⁻¹; Matsumoto et al. 2001; Kaaret et al. 2001) are intriguing, as they are apparently more luminous than the entire X-ray luminosity of a normal galaxy—with luminosities approaching that of luminous active galactic nuclei (AGNs). H/ULXs appear variable (Fabianno et al. 2003), their peak luminosity often changing by more than an order of magnitude within months to years (Matsumoto et al. 2001; Strickland et al. 2001). Here, we report an extraordinary HLX, as well as

more than a dozen ULXs, located within and along the same portion of the active star-forming outer ring of the Cartwheel.

The Cartwheel galaxy has been studied in the radio (Higdon 1996), IR (Marcum, Appleton, & Higdon 1992; Charmandaris et al. 1999), optical (Higdon 1995; Struck et al. 1996; Amram et al. 1998), and X-rays (Wolter, Trinchieri, & Iovino 1999). The crisp outer ring is believed to have been created as stars formed in radially expanding density waves caused by a companion (“intruder”) galaxy plunging through the center of a gas-rich disk (see Lynds & Toomre 1976; Toomre 1977; review by Appleton & Struck 1996). The outer ring appears to have propagated into a low-metallicity region of the disk (Fosbury & Hawarden 1977), where it has triggered recent active star formation.

Both H α and radio continuum observations (Higdon 1995, 1996) indicate that the dominant star-forming sites are in the outer ring of the southern quadrant, which constitutes about 80% of the total emission from the entire galaxy. *Chandra* observations discussed here clearly show that the dominant X-ray emission originates in the same starbursting southern ring quadrant.

2. IMAGING ANALYSIS AND SPECTRAL FITTING

The *Chandra* data analysis of the Cartwheel is part of a systematic, uniform archival study of nearly 20 interacting/merging galaxies. The Cartwheel was observed by ACIS-S (observation ID: 2019, PI: A. Wolter) with a 75 ks exposure from 2001 May 26 to 27. Data calibration was performed with CIAO version 2.3 using the latest calibration database. Events files of level one were obtained from the *Chandra* archive and were corrected for the aspect offset before processing into level two. Bad pixels and background flares as well as streaks were removed, and final clean maps were created. Further data analysis and image processing were done in IDL. This includes source detection, images of individual bands, and image smoothing (see Wang, Chaves, & Irwin 2003). We also followed various CIAO threads to extract the X-ray spectra for pointlike and extended sources. Spectral fitting was done with XSPEC. We also ran the timing analysis,

¹ Department of Astronomy, University of Massachusetts, LGRT-B 619E, 710 North Pleasant Street, Amherst, MA 01003-9305.

² Space Infrared Telescope Facility Science Center, California Institute of Technology, MS 220-6, 1200 East California Boulevard, Pasadena, CA 91125.

³ Space Telescope Science Institute, 3700 San Martin Drive, Baltimore, MD 21218.

⁴ $H_0 = 75$ km s⁻¹ Mpc⁻¹ ($cz = 9090$ km s⁻¹, $d_L = 122$ Mpc) is used in this Letter.

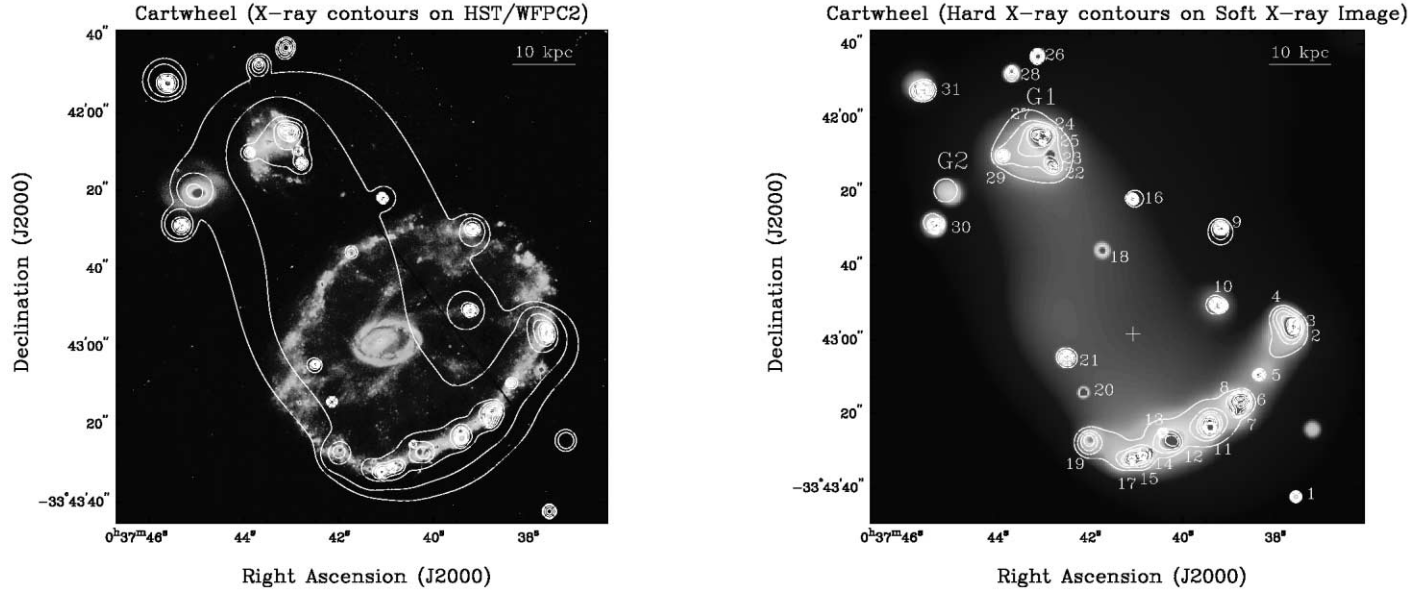


FIG. 1.—*Left*: Broadband X-ray contours overlaid on the *HST*/WFPC2 optical image. The lowest contours are 0.0345, 0.0431 counts pixel⁻¹ (pixel = $\sim 0''.5$) and then increase successively by a factor of 2. *Right*: Soft (0.3–1.5 keV) X-ray image overlaid with the hard X-ray contours (1.5–7 keV) with sources labeled. Companion galaxies G1 and G2 are labeled as well. The third companion galaxy G3 is $\sim 3'$ in the northeast, outside the region shown in the figure. [See the electronic edition of the *Journal* for a color version of this figure.]

TABLE 1
POINTLIKE X-RAY SOURCES (H/ULXs) IN THE
CARTWHEEL GALAXY SYSTEM

Number	CXO Name	Count Rate (counts ks ⁻¹)	H α ID ^a	Offset (arcsec)
1	J003737.56–334342.7	0.13 \pm 0.05
2	J003737.59–334257.3	2.11 \pm 0.21	CW-26	2.5
3	J003737.61–334255.8	1.91 \pm 0.19	CW-27	3.1
4	J003737.87–334253.6	0.16 \pm 0.06
5	J003738.36–334309.3	0.24 \pm 0.07	CW-25	3.0
6	J003738.75–334316.7	1.28 \pm 0.15	CW-24	1.4
7	J003738.82–334319.1	0.72 \pm 0.12	CW-23	0.7
8	J003738.97–334317.5	0.16 \pm 0.06
9	J003739.16–334230.9	0.60 \pm 0.10	CW-29	1.3
10	J003739.22–334250.6	0.96 \pm 0.13
11	J003739.40–334323.7	5.75 \pm 0.31	CW-20	1.7
12	J003740.26–334317.5	0.28 \pm 0.07	CW-17	1.4
13	J003740.46–334325.4	0.24 \pm 0.07
14	J003740.74–334330.7	0.35 \pm 0.08	CW-15	0.5
15	J003740.88–334331.3	1.04 \pm 0.13	CW-14	1.7
16	J003741.06–334221.9	0.31 \pm 0.08
17	J003741.09–334332.3	1.26 \pm 0.16	CW-12	1.6
18	J003741.73–334235.7	0.15 \pm 0.06	CW-3/4	2.3/2.7
19	J003742.01–334326.8	0.20 \pm 0.07	CW-10/9	1.8/0.7
20	J003742.15–334314.2	0.31 \pm 0.09
21	J003742.50–334304.5	0.33 \pm 0.08
22	J003742.80–334212.8	0.67 \pm 0.12
23	J003742.87–334210.2	0.32 \pm 0.08
24	J003742.96–334204.6	0.69 \pm 0.12
25	J003743.02–334206.3	0.84 \pm 0.13
26	J003743.13–334143.3	0.23 \pm 0.07
27	J003743.14–334204.4	1.13 \pm 0.15
28	J003743.70–334147.6	0.25 \pm 0.07
29	J003743.87–334210.2	0.67 \pm 0.11
30	J003745.32–334229.0	1.13 \pm 0.15
31	J003745.63–334152.3	4.91 \pm 0.33

^a H α knots as identified by Higdon (1995) with a point-spread function of $1''.7$ FWHM.

but none of the pointlike sources showed detectable variability within the observing time frame.

Figure 1 (*left*) shows broadband X-ray contours overlaid on a *Hubble Space Telescope* (*HST*)/Wide Field Planetary Camera 2 (WFPC2) *B*-band image. Almost all the X-ray emission in the Cartwheel originates from pointlike sources within the southern quadrant of the outer ring. The sources are nearly coincident with the strong H α , radio continuum emission, and blue superstar clusters (SSCs). Other portions of the outer ring show little X-ray emission except where exceptionally bright SSCs are seen. We label all the pointlike sources in the immediate surroundings of the Cartwheel in Figure 1 (*right*) and detail them in Table 1.

The companion galaxy G1 (spiral) contains six pointlike X-ray sources, and the early-type spiral G2 is seen as a fainter diffuse source (Fig. 1). The farthest companion galaxy G3 is also significantly detected, with one ULX in the eastern edge of its disk. In addition, a faint diffuse X-ray envelope that includes the Cartwheel, G1, and G2 is marginally detected.

The absence of any pointlike X-ray source in the nuclear region of the Cartwheel rules out the existence of an AGN. Although rather complex optical structures (Struck et al. 1996) and prominent mid-IR emission (Charmandaris et al. 1999) are in the inner disk/ring, the X-ray emission from Cartwheel's inner disk, including the nucleus, is extremely weak.

Table 2 summarizes our spectral fitting. For the strongest, source 11, both an absorbed Raymond-Smith (RS) and MEKAL thermal plasma models failed to yield the acceptable fit, giving an unrealistically high temperature, ≥ 10 keV, for the plasma. The absorbed power-law (PO) and multicolor accretion disk (MCD) models are both acceptable, but the data show excess emission features around 1.4 keV. This appears

TABLE 2
SPECTRAL FITTING AND MEASUREMENTS OF THE CARTWHEEL

Source	N_H (10^{21} cm^{-2})	Γ^a, T^b	χ^2/dof	$L_{2-10 \text{ keV}}$ ($10^{41} \text{ ergs s}^{-1}$)	$L_{0.5-10 \text{ keV}}$ ($10^{41} \text{ ergs s}^{-1}$)	$L_{0.05-100 \text{ keV}}$ ($10^{41} \text{ ergs s}^{-1}$)
HLX	3.5 ± 0.7	$1.6 \pm 0.2, \dots$ (PO)	17.5/21	0.8	1.3	4.1
HLX	2.0 ± 0.5	$\dots, 1.5 \pm 0.2$ (MCD)	16.4/21	0.6	0.9	1.0
HLX	2.6 ± 0.9	$1.4 \pm 0.2, 1.4 \pm 0.1$ (PO+Gau)	11.2/18	0.9	1.2	5.5
HLX	1.6 ± 0.5	$\dots, 1.7 \pm 0.4/1.4 \pm 0.1$ (MCD+Gau)	9.5/18	0.6	0.9	1.0
South ring	3.7 ± 1.9	$2.2 \pm 0.3, 0.18 \pm 0.02$ (PO+RS)	22.0/23	1.1	3.8	12.5
All ^c	1.8 ± 2.6	$2.3 \pm 0.9, 0.23 \pm 0.15$ (PO+RS)	6.2/12	.24	.53	2.6

^a PO, RS, Gau, and MCD are the power-law, RS thermal plasma, Gaussian emission line, and multicolor accretion disk models, respectively.

^b Γ is the photon index; T is the temperature in units of keV.

^c The diffuse emission from Cartwheel, G1, and G2 and between them. But all pointlike sources are excluded.

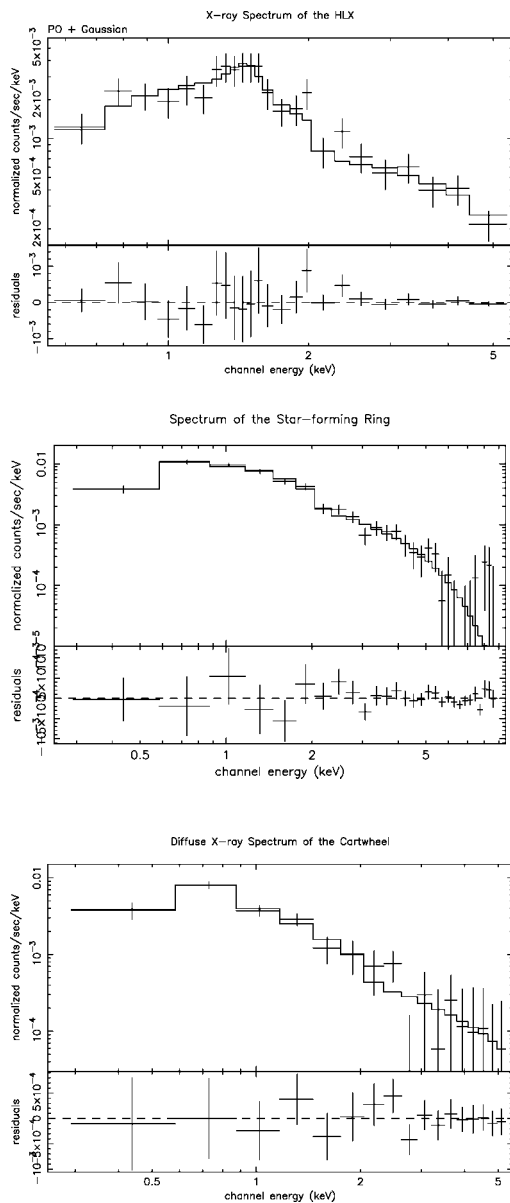


FIG. 2.—*Top*: Extracted X-ray spectra of the HLX and fitted with the absorbed PO plus Gaussian line features at 1.4 keV. *Middle*: The entire ring of southern quadrant. *Bottom*: The diffuse emission of the entire system with pointlike sources subtracted. The fits in the middle and bottom panels are the absorbed PO plus RS thermal plasma models (Table 2).

to be similar to the line features (Mg xi and Mg xiii) observed in a few ULXs in the Antennae (Zezas et al. 2002). We thus modeled the spectrum with an additional narrow Gaussian (Gau) component to the PO (Fig. 2, *top*) and MCD models. Both can give improved fit to the data.

Assuming isotropic emission, the absorption-corrected hard and broadband X-ray luminosities $L_{2-10 \text{ keV}}$ and $L_{0.5-10 \text{ keV}}$ of source 11 are $\sim 0.6\text{--}0.9$ and $0.9\text{--}1.3 \times 10^{41} \text{ ergs s}^{-1}$, respectively. Thus, this source is an HLX and could have a total luminosity $L_{0.05-100 \text{ keV}}$ as large as $\sim 5.0 \times 10^{41} \text{ ergs s}^{-1}$. In comparison, *ROSAT* data suggest an intrinsic $L_{0.5-5 \text{ keV}} \sim 2.3 \times 10^{41} \text{ ergs s}^{-1}$ for the detected outer ring assuming $N_H = 2 \times 10^{21} \text{ cm}^{-2}$ (Wolter et al. 1999), and most of the emission detected by *ROSAT* is presumably from source 11.

The whole southern ring, including diffuse emission and all the sources, taken together, can be fitted well with an absorbed PO+RS model. So can the diffuse emission of the entire system (Fig. 2, *middle and bottom*; Table 2). The unabsorbed hard and broadband X-ray luminosities of the south ring are 1.1 and $3.8 \times 10^{41} \text{ ergs s}^{-1}$. The total luminosity $L_{0.05-100 \text{ keV}}$ is as large as $1.2 \times 10^{42} \text{ ergs s}^{-1}$. Therefore, on average, all detected pointlike sources in the south ring would truly be ULXs, more luminous than the *most luminous* ULXs ($L_{0.5-10 \text{ keV}} \sim 6 \times 10^{39} \text{ ergs s}^{-1}$) detected in the Antennae. Although detailed spectral analysis is difficult for each of these pointlike sources owing to the limited count statistics (~ 100 photons), we can roughly estimate the X-ray flux according to their count rates. For instance, each of the double ULXs (sources 2 and 3) in the northwest end of the south ring has a count rate only 3 times smaller than that of the HLX. Both of the double ULXs (sources 15 and 17) southeast of the HLX also have count rates only a factor of 5 lower than that of the HLX. Thus, in combination, these four ULXs might have X-ray luminosity comparable to that of the HLX. The faintest sources detected have a luminosity of $L_{0.5-10 \text{ keV}} \sim 3 \times 10^{39} \text{ ergs s}^{-1}$.

A pointlike source 31, $\sim 10 \text{ kpc}$ north of G2, is likely a background galaxy or AGN, as it has a faint optical counterpart in the *HST* image. The limited spectrum can be fitted by an absorbed PO with a photon index ~ 1.9 but a much less absorption column density $N_H \sim 0.5 \times 10^{21} \text{ cm}^{-2}$.

3. ACTIVE STAR-FORMING RING KNOTS AND THE H/ULXs

Most H/ULXs are located within the portion of the Cartwheel ring that is experiencing the most powerful current star formation. Few ULXs discovered so far have prominent optical

counterparts (e.g., Immler et al. 2003; Wu et al. 2001), but almost all H/ULXs in the Cartwheel are closely associated with giant complexes of H II regions and blue SSCs (Fig. 1, *left*).

Although the HLX lies within $\sim 10''$ of the strongest H α knot, CW-17, which is also the hot spot in radio and mid-IR (Higdon 1995; Charmandaris et al. 1999), it is not coincident with this strongest starburst. Rather, the HLX lies closer ($1''.7 \sim 1$ kpc) to the fainter H α feature CW-20. In contrast, CW-17 coincides with a much softer (and fainter) ULX source 12. Hence the HLX defies an absolute one-to-one correspondence with an optical knot, although it lies within the arc of bright H α and radio emission that characterizes this portion of the ring.

We also give cross-identifications from the position match between H/ULXs and H α knots in Table 1. All five strongest H α knots (CW-14, CW-15, CW-17, CW-24, and CW-25) with H α luminosity $\geq 1.3 \times 10^{41}$ ergs s $^{-1}$, 20 times more luminous than 30 Doradus (Wang 1999), are coincident with the H/ULXs within $1''.7$. Moreover, except for three ULXs (sources 10, 20, and 21) interior to the outer ring and others (e.g., source 16 and those near G1, G2) outside of the outer ring, all H/ULXs seem to have spatial correspondence with the ring of the giant H II region complex. Nevertheless, a number of fairly strong H II regions do not have corresponding X-ray sources.

The evidence that (1) the HLX lies close to an H II region, (2) all five of the strongest H α knots have corresponding ULXs, and (3) there are a large number of matches between H α knots and other ULXs in the narrowly defined ring leads to the conclusion that H/ULXs appear to be directly linked to the production and evolution of the short-lived massive stars in the Cartwheel.

4. NATURE OF H/ULXs

The Cartwheel is the record holder in hosting both the HLX and the largest number of the *most luminous* ULXs in one galaxy. It has been argued on observational and theoretical grounds (Appleton & Struck 1996; Bransford et al. 1998) that the triggering of newly formed stars in ring galaxies occurs approximately simultaneously as the wave propagates out through the disk—the outer ring representing the most recently formed stars, with representative ages less than 10^7 yr. In this picture, the ring represents the outermost progress of a wave that began at the disk center some 300 Myr previously, created by the central perturbation of the intruder, either G3 or G1 (Mihos & Hernquist 1994; Higdon 1996; Struck et al. 1996). The striking similarity between the X-ray source distribution and the young SSCs and H II regions suggests a strong causal

connection between them. The lack of radial spread in the ring X-ray sources (with the exception of the three interior sources) indicates that, like the star-forming ring, the X-ray sources are linked to the active star formation episode and their young (< 10 Myr) ages.

The two most likely sources of X-ray emission associated with massive young star-forming regions are probably supernovae (SNe) or extremely young SN remnants (SNRs) and the high-mass X-ray binaries (HMXBs). We can almost rule out low-mass X-ray binaries (LMXBs) as the significant sources for H/ULXs along the Cartwheel narrow ring, although intermediate-mass black holes (IMBHs; see review by Miller & Colbert 2003) are likely viable. It is conceivable that LMXBs and/or background sources could be responsible for the three ULXs interior to the ring. Three ULXs outside the Cartwheel with faint optical counterparts are likely background galaxies. We restrict ourselves here to the majority of H/ULXs in the ring.

The interaction between the expanding SN ejecta and the dense circumstellar medium of the progenitor massive star can produce high X-ray luminosity $\sim 10^{40}$ ergs s $^{-1}$ (e.g., Pooley et al. 2002). Therefore, such young SNRs are not like classical Cas-A and are extremely bright with hard X-ray spectra. Some ULXs seem close to being resolved by *Chandra* at $0''.5$ (300 pc) resolution, suggesting that each ULX may be a composite of several individual luminous SNRs. If we adopt an SN rate for the outer ring of $0.1\text{--}1$ yr $^{-1}$ derived from the nonthermal radio continuum (Higdon 1996) and a minimum age for the ring H II regions of 1 Myr, then we would predict a few times 10^5 SNRs created over this period. Assuming that the X-ray phase of young SNRs is very short-lived ($\leq 10^2$ yr), then we might predict a few tens of young SNRs in the outer ring based on the radio flux alone. The individual ULXs in the ring could plausibly be collections of several such young SNRs. ULXs 6–8, 12–15, and 17 (Fig. 1, *right*) may be in this category, being closely associated with radio hot spots. Source 21, which lies just inside the outer ring and has no H α emission but has radio emission, may also be associated with SNRs.

In contrast, the HLX has only weak extended emission in both H α and radio continuum. Its extreme X-ray luminosity would seem to disfavor young SNRs unless they are unusually bright. Spectral fitting (Fig. 2, *left*) also does not support an SNR scenario for the HLX, given that both absorbed PO and MCD models could fit the data, whereas the thermal plasma models failed. This source may be the best candidate for an HMXB and/or IMBH since the formation of a massive black hole in dense star clusters is possible (e.g., Rasio, Freitag, & Gürkan 2003).

REFERENCES

- Amram, P., Mendes de Oliveira, C., Boulesteix, J., & Balkowski, C. 1998, *A&A*, 330, 881
 Appleton, P. N., & Struck, C. 1996, *Fundam. Cosmic Phys.*, 16, 111
 Bransford, M., Appleton, P. N., Marston, A. P., & Charmandaris, V. 1998, *AJ*, 116, 2757
 Charmandaris, V., et al. 1999, *A&A*, 341, 69
 Colbert, E., Heckman, T., Ptak, A., & Strickland, D. 2003, *ApJ*, submitted (astro-ph/0305476)
 Fabbiano, G., Zezas, A., & Murray, S. S. 2001, *ApJ*, 554, 1035
 Fabbiano, G., et al. 2003, *ApJ*, 584, L5
 Fosbury, R. A. E., & Hawarden, T. G. 1977, *MNRAS*, 178, 473
 Higdon, J. L. 1995, *ApJ*, 455, 524
 ———. 1996, *ApJ*, 467, 241
 Immler, S., Wang, Q. D., Leonard, D. C., & Schlegel, E. M. 2003, *ApJ*, 595, 727
 Kaaret, P., et al. 2001, *MNRAS*, 321, L29
 Lira, P., et al. 2002, *MNRAS*, 330, 259
 Lynds, R., & Toomre, A. 1976, *ApJ*, 209, 382
 Makishima, K., et al. 2000, *ApJ*, 535, 632
 Marcum, P. M., Appleton, P. N., & Higdon, J. L. 1992, *ApJ*, 399, 57
 Matsumoto, H., et al. 2001, *ApJ*, 547, L25
 Mihos, J. C., & Hernquist, L. 1994, *ApJ*, 437, 611
 Miller, M. C., & Colbert, E. J. M. 2003, *Int. J. Mod. Phys.*, submitted (astro-ph/0308402)
 Pooley, D., et al. 2002, *ApJ*, 572, 932
 Rasio, F. A., Freitag, M., & Gürkan, M. A. 2003, in *Coevolution of Black Holes and Galaxies*, ed. L. C. Ho (Cambridge: Cambridge Univ. Press), in press (astro-ph/0304038)
 Strickland, D. K., et al. 2001, *ApJ*, 560, 707
 Struck, C., Appleton, P. N., Borne, K. D., & Lucas, R. 1996, *AJ*, 112, 1868
 Toomre, A. 1977, in *IAU Symp. 79, The Large-Scale Structure of the Universe*, ed. M. S. Longair & J. Einasto (Dordrecht: Reidel), 109
 Wang, Q. D. 1999, *ApJ*, 510, L139
 Wang, Q. D., Chaves, T., & Irwin, J. A. 2003, *ApJ*, in press (astro-ph/0308150)
 Wolter, A., Trinchieri, G., & Iovino, A. 1999, *A&A*, 342, 41
 Wu, H., Xue, S. J., Xia, X. Y., Deng, Z. G., & Mao, S. 2002, *ApJ*, 576, 738
 Zezas, A., Fabbiano, G., Rots, A. H., & Murray, S. S. 2002, *ApJS*, 142, 239